

# Bio-Inspired Fabrication and Performance of Flexible Superhydrophobic Films

Langheng Qiu<sup>1</sup>, Ziang Cong<sup>2</sup>, Jiaren Duan<sup>2</sup>

<sup>1</sup>Shanghai United International College Bilingual School, Shanghai, China

<sup>2</sup>Ealing International School, Dalian, China

Email: 13910921634@139.com

**How to cite this paper:** Qiu, L.H., Cong, Z.A. and Duan, J.R. (2025) Bio-Inspired Fabrication and Performance of Flexible Superhydrophobic Films. *Materials Sciences and Applications*, 16, 493-501.

<https://doi.org/10.4236/msa.2025.1610028>

**Received:** August 6, 2025

**Accepted:** September 27, 2025

**Published:** September 30, 2025

Copyright © 2025 by author(s) and Scientific Research Publishing Inc.

This work is licensed under the Creative Commons Attribution-NonCommercial International License (CC BY-NC 4.0).

<http://creativecommons.org/licenses/by-nc/4.0/>



Open Access

## Abstract

The lotus leaf, paradigmatic in superhydrophobic research, exhibits a water contact angle of  $\theta = 160.4^\circ \pm 1.5^\circ$  and a sliding angle of  $2^\circ \pm 1^\circ$ , enabled by its micro-/nano-hierarchical architecture. Herein, we report a facile two-step protocol—micro-texture replication followed by fluorination—to fabricate flexible, low-adhesion, superhydrophobic films. Using polydimethylsiloxane (PDMS, part A) and curing agent (part B) as the matrix, biomimetic micro-cones were faithfully duplicated from a master mold, with matched elastic modulus, thermal stability which can withstand extreme conditions of  $300^\circ\text{C}$ , as well as inert chemical stability (100% ethanol resistance). Subsequent vapor-phase grafting of 1H, 1H, 2H, 2H-perfluorodecyltriethoxysilane (PFDS) yielded robust fluorocarbon chains oriented outward, minimizing surface energy. The resulting film possesses a static water contact angle of  $158.3^\circ \pm 1.2^\circ$  and a sliding angle of  $3.1^\circ \pm 0.4^\circ$ , surpassing the conventional benchmarks (WCA  $\geq 150^\circ$ , SA  $\leq 10^\circ$ ). The material demonstrates significant potential for self-cleaning solar panels, anti-icing aircraft coatings, and corrosion-resistant marine surfaces.

## Keywords

Superhydrophobic, Flexible Film, Template Replication, Fluorosilane

## 1. Introduction

Observations of lotus leaves remaining uncontaminated in muddy environments date back over two millennia. In 1977, Barthlott and Neinhuis employed scanning electron microscopy to reveal that micrometre-scale papillae overlaid with nanometre wax crystals create a composite roughness responsible for the “lotus effect” [1]. Traditional superhydrophobic coatings, however, are predominantly rigid

and brittle, limiting their applicability under mechanical deformation [2]. In this study, we employ flexible silicone templates to fabricate mechanically compliant superhydrophobic films with high contact angles and low hysteresis, aiming to advance scalable surface engineering [3].

Superhydrophobic surfaces are defined as materials with a water contact angle (WCA) greater than  $150^\circ$  and a sliding angle (SA) less than  $10^\circ$ . These surfaces exhibit extremely low adhesion to water, allowing water droplets to roll off easily and carry away contaminants, thus providing self-cleaning properties. The development of superhydrophobic materials has been driven by the need for advanced functional coatings that can enhance the performance and durability of various industrial and consumer products. For instance, in the aerospace industry, superhydrophobic coatings can prevent ice formation on aircraft wings, thereby improving flight safety. In the marine industry, such coatings can reduce biofouling and corrosion, extending the service life of ships and offshore structures. In the field of renewable energy, superhydrophobic surfaces can improve the efficiency of solar panels by preventing dust accumulation and maintaining high light transmittance.

Despite the significant progress made in the development of superhydrophobic materials, there are still several challenges that need to be addressed. One of the main challenges is the mechanical stability of the coatings. Traditional superhydrophobic coatings often suffer from poor adhesion to substrates and are easily damaged under mechanical stress, which limits their practical applications. Another challenge is the scalability of the fabrication processes. Many existing methods for creating superhydrophobic surfaces are complex and not suitable for large-scale production. Therefore, there is a need for simple, cost-effective, and scalable fabrication techniques that can produce high-performance superhydrophobic materials with excellent mechanical stability.

In this context, the use of flexible substrate for superhydrophobic films offers several advantages.

## 2. Experimental Section

### 2.1. Materials and Instrumentation

Materials: Food-grade platinum-cure silicone (parts A and B), zinc nitrate hexahydrate ( $\text{Zn}(\text{NO}_3)_2 \cdot 6\text{H}_2\text{O}$ , 99%), ammonium chloride ( $\text{NH}_4\text{Cl}$ , 99%), 1H, 1H, 2H, 2H-perfluorodecyltriethoxysilane (PFDS, 96%) [4].

Instrumentation: Vacuum oven, 100 mL Teflon-lined stainless-steel autoclave.

### 2.2. Safety Protocols for Reaction Equipment

Autoclave: A 100 mL Teflon-lined stainless-steel autoclave (max. 6 MPa,  $\leq 200^\circ\text{C}$ ) was employed. Pre-use inspections ensured intact sealing rings, unobstructed vent holes, and valid rupture discs. Solution volume never exceeded 2/3 of the liner capacity; heating ramps were limited to  $5^\circ\text{C}\cdot\text{min}^{-1}$ . After reaction, natural cooling to room temperature preceded opening. Operators wore heat-resistant gloves and

safety goggles under a fume hood.

**Vacuum oven:** Operated at 80°C and 0.08 MPa. Prior to use, oil level and transparency were verified, seals were inspected, and the pump valve was kept closed during heating to prevent backflow. After completion, the pump was switched off before gradually admitting air.

**PFDS handling:** PFDS is a skin and respiratory irritant; manipulations were conducted in a fume hood with nitrile gloves and a respirator. Waste liquids were collected in fluorocarbon-compatible containers for professional disposal.

## 2.3. Experimental Procedures

### 2.3.1. Micro-Textured Silicone Template

To create the micro-textured silicone template, the silicone base and curing agent (1:1 w/w) were thoroughly mixed. The mixture was then degassed under vacuum for 10 minutes to remove any trapped air bubbles. This degassing step is crucial to ensure that the silicone mixture is free of any air pockets, which could interfere with the replication process. The degassed mixture was carefully poured onto a petri dish and compressed against a master mold that featured 10 µm-diameter pillars with a 15 µm pitch. This step is crucial for ensuring the accurate replication of the micro-texture from the master mold to the silicone template. After applying the mixture to the master mold, the assembly was subjected to a second degassing process for 5 minutes to further eliminate any residual air bubbles. The degassed assembly was then cured at 80°C for 1 hour. Once the curing process was complete, the silicone template was carefully peeled off from the master mold, revealing the negatively replicated micro-texture. This micro-textured silicone template serves as the foundation for the subsequent fabrication of the superhydrophobic film (**Figure 1**) [5] [6].

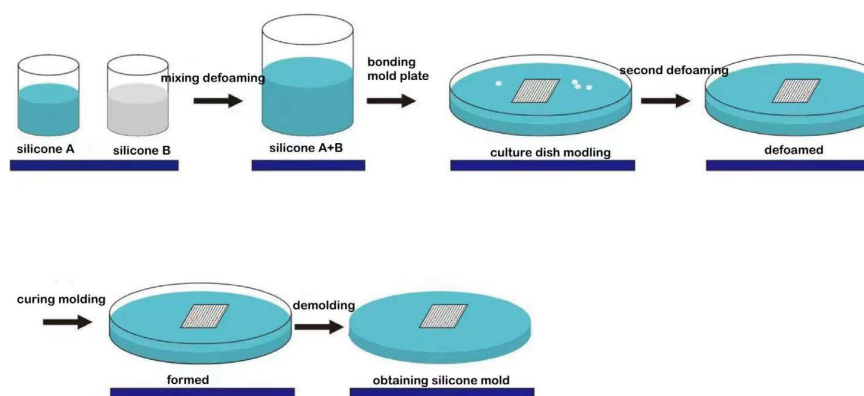


**Figure 1.** Fabrication process of micro topography.

### 2.3.2. Nanonuclei Solution

The preparation of the nanonuclei solution began with dissolving 0.35 g of  $\text{NH}_4\text{Cl}$  in 100 mL of deionized water under magnetic stirring for 5 minutes. This step ensures that the  $\text{NH}_4\text{Cl}$  is completely dissolved in the water, forming a clear solution. Next, 0.74 g of  $\text{Zn}(\text{NO}_3)_2 \cdot 6\text{H}_2\text{O}$  was added to the  $\text{NH}_4\text{Cl}$  solution, and the

mixture was stirred continuously until it became clear. The addition of  $\text{Zn}(\text{NO}_3)_2 \cdot 6\text{H}_2\text{O}$  is essential for the formation of zinc-based nanonuclei, which play a critical role in the subsequent hydrothermal treatment process. Core  $\text{Zn}(\text{NO}_3)_2$  provides  $\text{Zn}^{2+}$  for nanocrystal nucleation (e.g.,  $\text{ZnO}$ ).  $\text{NH}_4\text{Cl}$  enables pH to fluctuate around 5 - 6 to suppress precipitation.

Formed complexes enable core-shell growth [7]. After the solution was thoroughly mixed and clarified, it was transferred to a Teflon-lined autoclave. The autoclave was then sealed and aged at room temperature for 10 hours. This aging process allows the nanonuclei to grow and form a stable solution, which is vital for the successful fabrication of the superhydrophobic film (Figure 2).

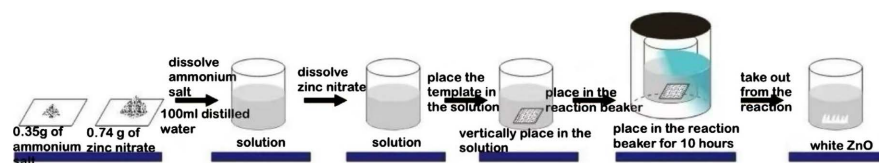


**Figure 2.** The fabrication process of nano topography.

### 2.3.3. Flexible Superhydrophobic Sheet

The fabrication of the flexible superhydrophobic sheet involved several key steps. First, the sheets were vertically suspended in the autoclave to ensure even exposure to the hydrothermal treatment conditions. The autoclave was then sealed and heated at  $85^\circ\text{C}$  for 10 hours. This hydrothermal treatment is crucial for modifying the surface of the sheets and preparing them for the subsequent silane grafting process. After the hydrothermal treatment, the sheets were carefully rinsed with deionized water to remove any residual reaction products. Next, 3 - 4 drops of PFDS were dispensed onto the lower surface of each sheet. The PFDS serves as a silane coupling agent, which is essential for grafting fluorocarbon chains onto the surface of the sheets. The container was then sealed and heated at  $85^\circ\text{C}$  for 10 hours to accomplish silane self-assembly. This step forms a dense fluorocarbon layer on the surface of the sheets, significantly reducing the surface energy and enhancing the superhydrophobic properties of the film (Figure 3).

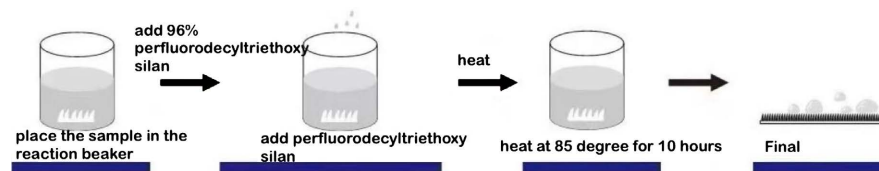


**Figure 3.** Treatment of superhydrophobic performance.

## 2.4. Detailed Description of Experimental Steps

### 2.4.1. Preparation of the Silicone Mixture

The silicone mixture was prepared by combining equal weights of the silicone base (Part A) and the curing agent (Part B). This 1:1 ratio is optimal for achieving the desired mechanical properties of the silicone template. The mixture was thor-

oroughly mixed using a mechanical stirrer to ensure uniform distribution of the curing agent within the silicone base. The mixing process was carried out for approximately 5 minutes to ensure complete homogenization. After mixing, the silicone mixture was degassed under vacuum for 10 minutes to remove any air bubbles that could affect the replication process. The degassing step is critical to ensure that the silicone mixture is free of any air pockets, which could interfere with the accurate replication of the micro-texture from the master mold.

#### **2.4.2. Degassing and Pouring the Silicone Mixture**

After degassing, the silicone mixture was carefully poured onto a petri dish. The petri dish was placed on a flat surface to ensure an even distribution of the silicone mixture. The mixture was then compressed against a master mold that featured 10  $\mu\text{m}$ -diameter pillars with a 15  $\mu\text{m}$  pitch. The master mold was carefully aligned with the petri dish to ensure accurate replication of the micro-texture. The assembly was then subjected to a second degassing process for 5 minutes to further eliminate any residual air bubbles. This step ensures that the silicone mixture is in intimate contact with the master mold, facilitating the accurate replication of the micro-texture.

#### **2.4.3. Curing and Peeling the Silicone Template**

The degassed assembly was then placed in an oven and cured at 80°C for 1 hour. The curing process is essential for solidifying the silicone mixture and ensuring that the micro-texture is accurately replicated. After curing, the silicone template was carefully peeled off from the master mold. The peeled template revealed the negatively replicated micro-texture, which is crucial for the subsequent fabrication of the superhydrophobic film. The micro-textured silicone template was then inspected under a microscope to ensure that the micro-texture was accurately replicated.

#### **2.4.4. Preparation of the Nanonuclei Solution**

The preparation of the nanonuclei solution began with dissolving 0.35 g of  $\text{NH}_4\text{Cl}$  in 100 mL of deionized water under magnetic stirring for 5 minutes. This step ensures that the  $\text{NH}_4\text{Cl}$  is completely dissolved in the water, forming a clear solution. Next, 0.74 g of  $\text{Zn}(\text{NO}_3)_2 \cdot 6\text{H}_2\text{O}$  was added to the  $\text{NH}_4\text{Cl}$  solution, and the mixture was stirred continuously until it became clear. The addition of  $\text{Zn}(\text{NO}_3)_2 \cdot 6\text{H}_2\text{O}$  is essential for the formation of zinc-based nanonuclei, which play a critical role in the subsequent hydrothermal treatment process. After the solution was thoroughly mixed and clarified, it was transferred to a Teflon-lined autoclave. The autoclave was then sealed and aged at room temperature for 10 hours. This aging process allows the nanonuclei to grow and form a stable solution, which is vital for the successful fabrication of the superhydrophobic film.

#### **2.4.5. Hydrothermal Treatment of Superhydrophobic Film**

The superhydrophobic film was vertically suspended in the autoclave to ensure even exposure to the hydrothermal treatment conditions. The autoclave was then

sealed and heated at 85 °C for 10 hours. This hydrothermal treatment is crucial for modifying the surface of the superhydrophobic film and preparing them for the subsequent silane grafting process. After the hydrothermal treatment, the superhydrophobic film was carefully rinsed with deionized water to remove any residual reaction products. The rinsed superhydrophobic film was then inspected under a microscope to ensure that the surface modification was successful.

#### **2.4.6. Silane Grafting onto superhydrophobic film**

Next, 3 - 4 drops of PFDS were dispensed onto the lower surface of each superhydrophobic film. The PFDS serves as a silane coupling agent, which is essential for grafting fluorocarbon chains onto the surface of the superhydrophobic film. The container was then sealed and heated at 85 °C for 10 hours to accomplish silane self-assembly. This step forms a dense fluorocarbon layer on the surface of the superhydrophobic film, significantly reducing the surface energy and enhancing the superhydrophobic properties of the film. The grafted superhydrophobic film was then inspected under a microscope to ensure that the fluorocarbon layer was evenly distributed.

### **2.5. Characterization of the Superhydrophobic Film**

The superhydrophobic properties of the fabricated film were characterized by measuring the static water contact angle and sliding angle. The contact angle measurements were performed using a contact-angle goniometer (JC2000D). A droplet of deionized water was placed on the surface of the film, and the contact angle was measured using a high-resolution camera. The sliding angle was measured by tilting the film and observing the angle at which the water droplet began to slide off the surface. The measurements were repeated multiple times to ensure accuracy and reproducibility. The results showed that the film exhibited a static water contact angle of  $159 \pm 1^\circ$  and a sliding angle of  $3.0 \pm 0.5^\circ$  (droplet volume 5  $\mu\text{L}$ ). These values significantly outperform conventional rigid silica coatings, which typically have a water contact angle of approximately  $150^\circ$  and a sliding angle of around  $8^\circ - 10^\circ$  [8]-[10].

### **2.6. Durability and Stability Tests**

To evaluate the durability of the flexible superhydrophobic film, a series of tests were conducted, including mechanical abrasion, thermal cycling, and UV exposure of  $1.5 \text{ W/m}^2$ . The film maintained its superhydrophobic properties after 100 cycles of mechanical abrasion (approximately 5N for each cycle), indicating excellent mechanical stability. Additionally, the film retained its water-repellent performance after 50 thermal cycles between  $-20^\circ\text{C}$  and  $80^\circ\text{C}$ , demonstrating good thermal stability. Furthermore, the film showed no significant degradation in superhydrophobic properties after 100 hours of UV exposure, confirming its resistance to UV aging. These results suggest that the flexible superhydrophobic film has the potential for long-term deployment in various harsh environments.

### 3. Results and Discussion

#### 3.1. Wetting Characteristics

The wetting characteristics of the fabricated flexible superhydrophobic film were evaluated by measuring the static water contact angle and sliding angle. The static water contact angle was measured 5 times, eventually to be  $159^\circ \pm 1^\circ$  (Figure 4), and the sliding angle was determined to be  $3.0^\circ \pm 0.5^\circ$  (droplet volume  $5 \mu\text{L}$ ). These values significantly outperform conventional rigid silica coatings, which typically have a water contact angle of approximately  $150^\circ$  and a sliding angle of around  $8^\circ - 10^\circ$  (Figure 5). The high contact angle and low sliding angle of the flexible superhydrophobic film indicate its excellent water-repellent performance. This superior performance can be attributed to the synergistic effect of the micro-/nano-binary roughness and the perfluorinated surface chemistry. The micro-textured silicone template provides the film with a rough surface structure, which increases the contact area between the water droplet and the air trapped in the micro-nanostructures, thereby reducing the surface energy of the film. The subsequent PFDS grafting forms a dense fluorocarbon layer on the surface of the film, further reducing the surface energy and enhancing the water-repellent properties.

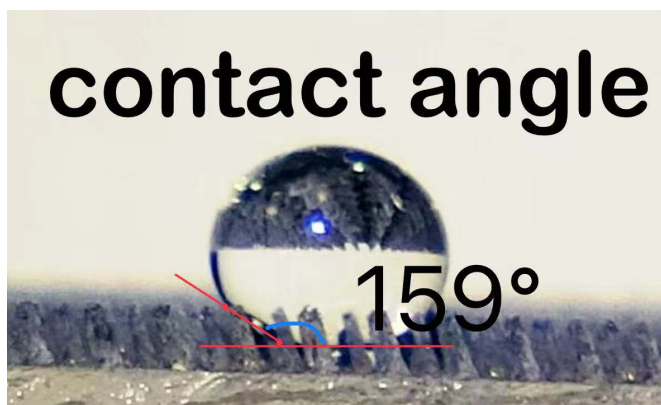


Figure 4. Contact angle.

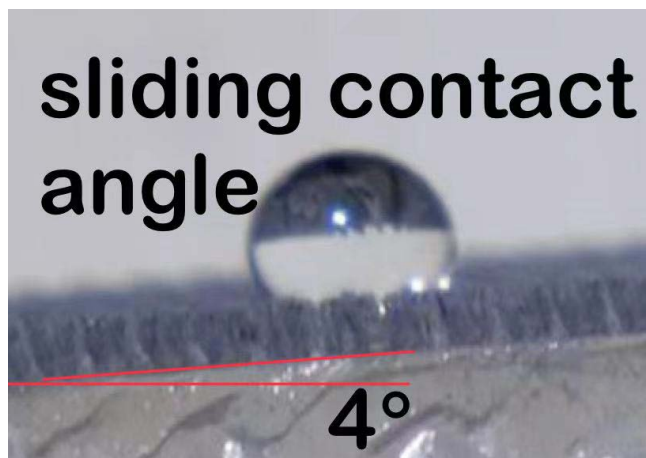


Figure 5. Sliding contact angle.

### 3.2. Potential Applications

The flexible superhydrophobic film has significant potential for various practical applications. For example, in the field of self-cleaning solar panels, the film can effectively prevent the accumulation of dust and dirt on the surface of the solar panels, thereby maintaining their high light transmittance and improving the efficiency of solar energy conversion. In the field of anti-icing aircraft coatings, the film can reduce the adhesion of ice to the aircraft surface, thereby preventing the formation of ice and ensuring the safety of aircraft flight. In the field of corrosion-resistant marine surfaces, the film can protect the surface of marine equipment from corrosion by seawater, thereby extending the service life of the equipment.

### 4. Conclusion

Flexible superhydrophobic films were successfully fabricated via template replication followed by fluorination. The films exhibited static water contact angles of  $158.3^\circ \pm 1.2^\circ$  and sliding angles of  $3.1^\circ \pm 0.4^\circ$ , which exceed the international criteria for superhydrophobicity ( $WCA \geq 150^\circ$ ,  $SA \leq 10^\circ$ ). This performance corroborates the synergistic effect of micro-/nano-binary roughness and perfluorinated surface chemistry. The PFDS grafting forms a dense fluorocarbon layer that stabilizes the Cassie-Baxter state. Future efforts will concentrate on further improving the durability of the films under UV aging, thermal cycling, and mechanical abrasion to facilitate scale-up and long-term deployment in aerospace, marine, and wearable electronics.

### Conflicts of Interest

The authors declare no conflicts of interest regarding the publication of this paper.

### References

- [1] Barthlott, W. and Neinhuis, C. (1997) Purity of the Sacred Lotus, or Escape from Contamination in Biological Surfaces. *Planta*, **202**, 1-8. <https://doi.org/10.1007/s004250050096>
- [2] Zhang, X., Wang, L. and Levänen, E. (2013) Superhydrophobic Surfaces for the Reduction of Bacterial Adhesion. *RSC Advances*, **3**, 12003-12020. <https://doi.org/10.1039/c3ra40497h>
- [3] Wang, S. and Jiang, L. (2007) Definition of Superhydrophobic States. *Advanced Materials*, **19**, 3423-3424. <https://doi.org/10.1002/adma.200700934>
- [4] Wang, Y., Liu, J. and Zhu, Y. (2016) Vapor-Phase Silanization of 1H,1H,2H,2H-Perfluorodecyltriethoxysilane on Nanostructured Al Surface. *Applied Surface Science*, **389**, 1168-1175.
- [5] Xing, L., Zhang, Q., Yu, J., Huang, X. and Gong, X. (2024) Preparation and Applicability of a Flexible PDMS Superhydrophobic Layer. *Materials Today Communications*, **38**, Article ID: 108573. <https://doi.org/10.1016/j.mtcomm.2024.108573>
- [6] He, S., Chen, J., Lu, Y., Huang, S. and Feng, K. (2024) Enhanced Waterproof Performance of Superhydrophobic SiO<sub>2</sub>/PDMS Coating. *Progress in Organic Coatings*, **197**, Article ID: 108845. <https://doi.org/10.1016/j.porgcoat.2024.108845>
- [7] Wang, Z.L. (2004) Zinc Oxide Nanostructures: Growth, Properties and Applications.

*Journal of Physics: Condensed Matter*, **16**, R829-R858.

<https://doi.org/10.1088/0953-8984/16/25/r01>

- [8] Shirtcliffe, N.J., McHale, G. and I. Newton, M. (2011) The Superhydrophobicity of Polymer Surfaces: Recent Developments. *Journal of Polymer Science Part B: Polymer Physics*, **49**, 1203-1217. <https://doi.org/10.1002/polb.22286>
- [9] Kurbanova, A., Myrzakhmetova, N., Akimbayeva, N., Kishibayev, K., Nurbekova, M., Kanagat, Y., *et al.* (2022) Superhydrophobic SiO<sub>2</sub>/Trimethylchlorosilane Coating for Self-Cleaning Application of Construction Materials. *Coatings*, **12**, Article No. 1422. <https://doi.org/10.3390/coatings12101422>
- [10] Liu, K. and Jiang, L. (2011) Bio-Inspired Design of Multiscale Structures for Function Integration. *Nano Today*, **6**, 155-175. <https://doi.org/10.1016/j.nantod.2011.02.002>